Electronic Supplementary Material (ESI) for ChemComm.

Supporting Information

Cu-Zn nanoparticles promoter for selective carbon dioxide reduction and its application for visible-light-active Z-scheme system using water as electron donor

Ge Yin,[a] Hiroshi Sako,[a] Gubbala V. Ramesh,[b] Shigenori Ueda,[c] Akira Yamaguchi,[a] Hideki Abe,[b, *] and Masahiro Miyauchi[a, *]

This supporting information contains (I) the details of the experimental and evaluation methods. (II) characterization, optimization and evaluation of Cu-Zn NPs. (III) the characterization of the light harvesters and (IV)photocatalytic performance of the CFO/WO_3 system.

(I) Experimental details

Preparation of Cu-Zn nanoparticles ink. Intermetallic Cu-Zn nanoparticles were synthesized by chemical co-reduction of metal precursors in diglyme. Copper acetate and zinc acetate were used as metal precursors. After precursors were weighed and put into vessel, diglyme was also added into the vessel as solvent and the mixture was stirred for 1 min. Then super-hydride solution 1.0 M lithium triethylborohydride in THF ($LiBH_4(C_2H_3)_5$) was added into the reaction as reducing agent. The mixture was then heated at 200 ˚C using oil bath for 2 hours. The products were separated by centrifuging and washed by hexane, and dried under vacuum, then the Cu-Zn nanoparticles were collected.

During the preparation, all the operation was conducted under Ar atmosphere or vacuum condition. All the agents were anhydrous to prevent the nanoparticles formation by oxidation.

4 mg of Cu-Zn nanoparticles were then dispersed in isopropanol (IPA) solution (440 µl IPA in 1745 µl water), with small amount of nafion (22µl) inside. A highly dispersed Cu-Zn ink was made by ultra sonication for 1 hour. It should be noticed that the Cu-Zn nanoparticles can be easily oxidized in the ink, so the ink should be freshly-made before every experiment. The Cu-Zn NPs ink can be easily taken as needed amount and drop

on the substrates and dried by keeping in vacuum desiccators. In the case of electrochemical evaluation, the substrate was pure Ti metal sheet, while in the case of photoelectrochemical cell, the substrate was $CaFe_2O_4$ electrode.

Preparation of $SrTiO_3$ film. A $SrTiO_3$ paste was made from $SrTiO_3$ nanopowders from Wako Ltd. Fluorine doped tin oxide (FTO) glass was used as a substrate, $SrTiO_3$ film (2 x 2cm^2) was screen printed on a FTO glass, and annealed under 450 ˚C for 1 hour.

Preparation of $CaFe_2O_4$(CFO) electrode. The CFO powder was prepared by a solution method referring from the previous literature.[14, 17] Calcium acetate monohydrate ($(CH_3COO)_2Ca{\cdot}H_2O$, 99%, Wako Pure Chemical Industries, Ltd.) and Iron (III) nitrate nonahydrate, ($Fe(NO_3)_3{\cdot}9H_2O$, 99.9 %, Wako Pure Chemical Industries, Ltd.) were used as precursors. After these precursors were weighed and dissolved in water, polyethylene glycol (5 wt%) was added into the solution. After heating at 120˚C with stirring, dry powders were collected and then annealed at 450 ˚C for 2 hours and 1050 ˚C for 10 hours. To prepare the CFO electrode, the synthesized CFO powder was made into a paste, by fully mixing with ethyl cellulose and α-terphenol, and then printed onto a pure metal substrate by screening printing method. The CFO printed film was heated under 450 ˚C for 2 h to remove the contamination, then heated up to 1250 ˚C for 2h to crystallize CFO.

Preparation of WO_3 nanotree electrode. The WO_3 nanotree film was fabricated on a metal tungsten substrate by a facile hydrothermal synthesis. The metal tungsten substrate (0.5-mm thickness, Niraco) was cut into 2cm × 2cm squares and then annealed in air at 500 ˚C for 1 h to oxidize the film. For hydrothermal treatment, the oxidized tungsten metal plates were placed in an aqueous solution of 0.2 M nitric acid (HNO_3, 25 mL) containing oxalic acid ($H_2C_2O_4$, 1.56 g) and rubidium sulfate (Rb_2SO_4, 0.2 g), and heated at 150 ˚C for 30 hours in an autoclave. After the hydrothermal reaction, the substrates were gently washed with 1M HNO_3 solution and pure water, and then dried using Ar gas gun immediately. The dried samples were annealed in air at 700 ˚C for 1 h for oxidation to decrease oxygen defects in WO_3. For photoelectrochemical evaluation, a copper wire was attached to the back side of WO_3 electrode using silver paste. The copper wire and exposed metal substrate were covered with an epoxy resin, leaving only the surface of the WO_3 nanotrees exposed.

The construction of H-type photoelectrochemical cell. A H-type glass cell was used for the photoelectrochemical evaluation. The Cu-Zn NPs loaded CFO electrode was used as a cathode, and the WO_3 nanotree electrode was used as a photoanode (Figure S1 in the supporting information). The cathodic- and anodic sides of the glass cell were separated by a Nafion membrane. The electrolyte on the cathodic side was a CO_2-purged 0.1 M $KHCO_3$ and 0.1M KOH solution and that on the anodic side was a N_2-purged 0.1 M KCl solution. During the performance tests, both the cathodic and anodic sides were irradiated by visible light, whose spectrum was shown in Figure. S2. The gaseous products in the headspace such as CH_4, CO, and H_2 were quantified with a gas chromatograph (BID, SHIMADZU). The liquid products in the electrolyte solution such as HCOOH were quantified with an ion chromatograph (Prominence Organic Acid Analyse System with pH buffered post column, not influenced by the matrix, SHIMADZU).

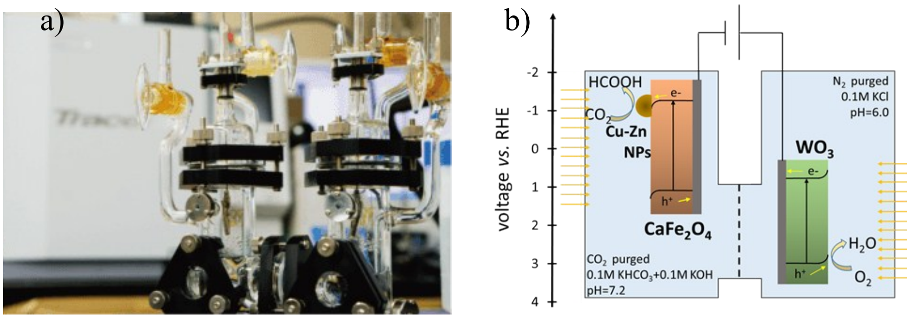

Figure S1. a) the highly air-tight H-type cell used in the present research, b) the construction and reaction mechanism of the H-type photoelectrochemical cell.

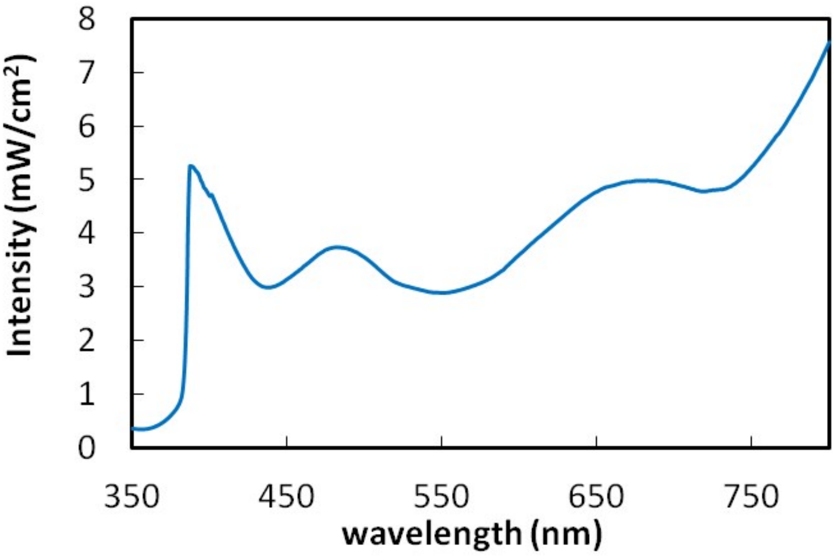

Figure S2. The light spectrum of the light source used in the photocatalytic evaluation.

Electrochemical CO_2 reduction. The prepared Cu-Zn coated Ti electrode was used as the working electrode, a pure Pt plate was used as counter electrode, and an Ag/AgCl electrode was used as reference electrode, respectively. CO_2 or Ar gasses were purged into the 0.1 M $KHCO_3$ electrolyte. To clean the contamination on the electrode surface, a cleaning process was operated under cyclic voltammetry condition: starting bias (E_0)= -0.9 V, 1st operating bias (E_1) = -1.8 V, and 2nd operating bias (E_2)= -0.1 V, with a slope of 90 mV/ sec. This cleaning procedure was repeated for 10 cycles of cyclic voltammogram under photon irradiation.

(II) Characterization, optimization and evaluation of Cu-Zn NPs.

Three kinds of Cu-Zn NPs were synthesized using metal precursors of Cu and Zn with molar ratio of 1:3, 3:1, and 1:1. According to the XRD patterns in Figure S3, the peak of Cu-Zn intermetallic was seen from the Cu-Zn NPs with Cu:Zn ratio of 3:1 and 1:1, but the peak was not seen in that of 1:3. Hard X-ray photoelectron spectroscopy (HAXPES) analyses were also operated, as shown in Figure S4, the Cu *2p* and Zn *2p* peak positions for the Cu-Zn NPs (3:1 and 1:1) shifted from those for pure Cu and Zn, indicating an intermetallic structure. But the shift of Cu-Zn NPs (1:3) was small.

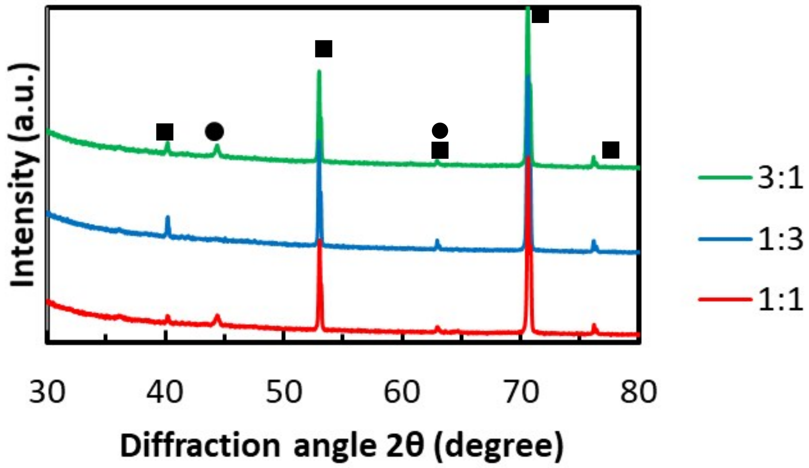

Figure S3. The XRD pattern of the Cu-Zn NPs, with different molar ratio of Cu and Zn, grafted on the surface of metal Ti sheet. ●: Cu$_5$Zn$_8$ (cubic), ■: pure Ti.

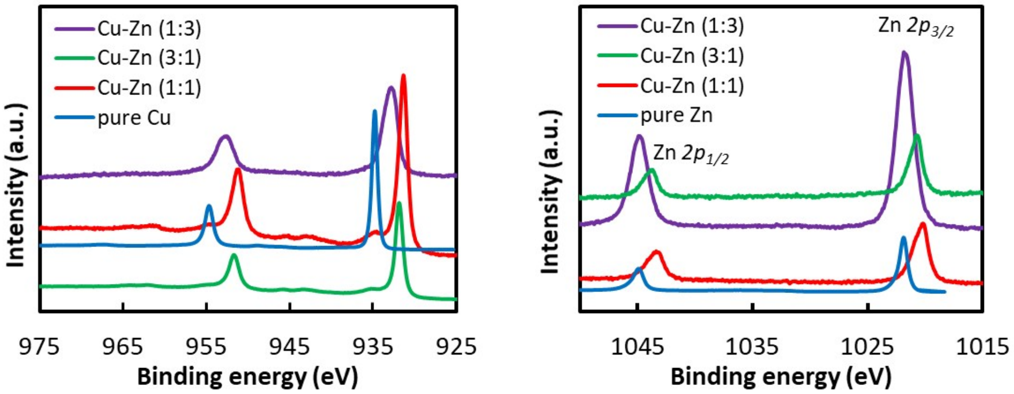

Figure S4. The HAXPES spectra of Cu *2p* and Zn *2p* core-levels in the prepared Cu-Zn alloy nanoparticles, comparing with those of pure Cu and pure Zn.

The electrocatalytic properties for CO_2 reduction of the synthesized Cu-Zn NPs were screened by electrochemical methods under dark condition. Cycle voltammogram (CV) curves of the prepared Cu-Zn NPs under CO_2 and N_2 atmosphere were analyzed, CV curves of pure Cu and pure Zn were also analyzed as control groups. As we can see from Figure S5, compared to the other two kinds, the NPs with Cu: Zn molar ratio of 1:1 exhibited the lowest onset potential of CO_2 reduction, and the current density of CO_2 atmosphere was higher than that of N_2 atmosphere. These results demonstrated that the Cu-Zn NPs behave best electrocatalytic properties when the Cu: Zn molar ratio equals to 1:1. Thus in the following researches, this optimized Cu-Zn NPs composition was used.

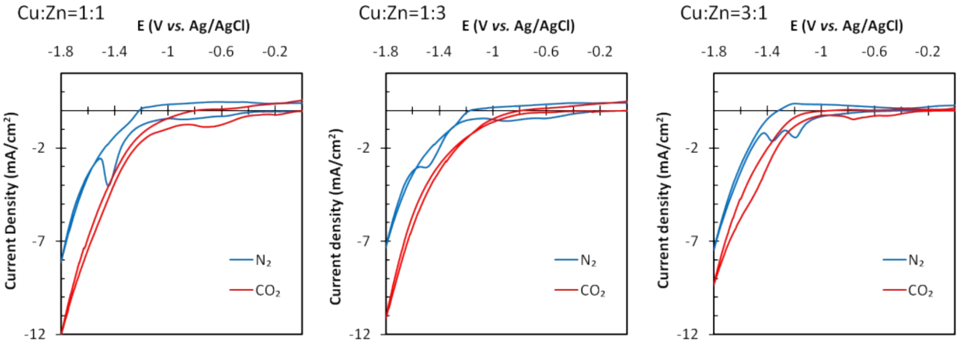

Figure S5. Cycle voltammetry (CV) curves of three kind of Cu-Zn NPs.

The Cu-Zn NPs (1:1) was characterized by TEM and EDX, as seen from Figure S6.

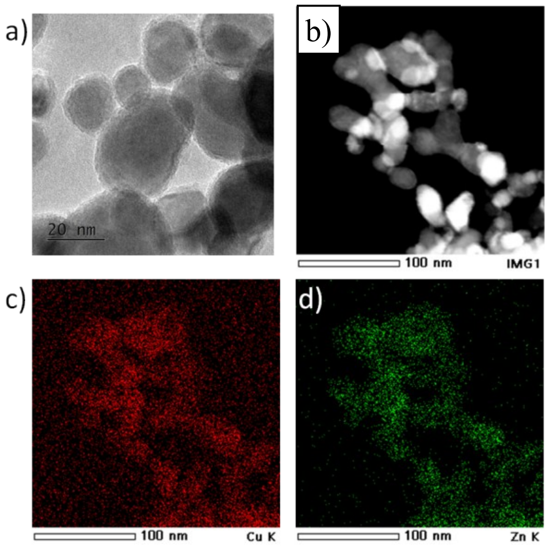

Figure S6. a) The TEM image and b), c), d) EDX analyses about the distribution of Cu and Zn in the Cu-Zn NPs (1:1).

The XRD pattern of the Cu-Zn NPs (1:1) proved that it has Cu_5Zn_8 intermetallic structure.

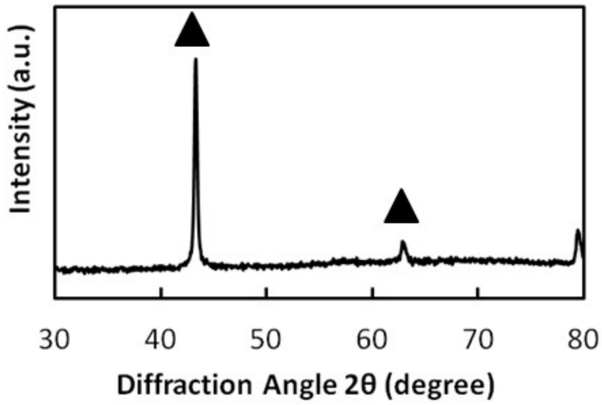

Figure S7. the XRD pattern of Cu-Zn NPs (1:1), ▲Cu_5Zn_8 (cubic).

The Cu-Zn NPs were coated on the pure Ti sheet and used as working electrode in a CO_2 purged electrochemical cell, the products generated under different bias-potential in 1 hour were detected, as shown in Figure S8, HCOOH was generated under high selectivity.

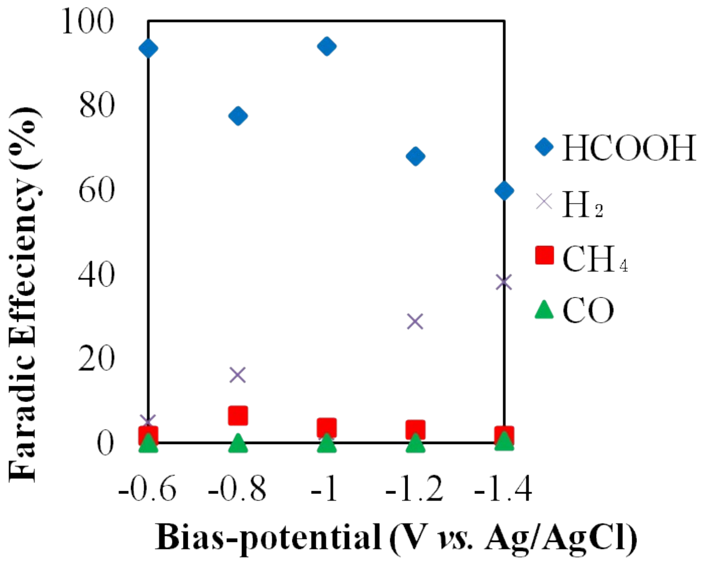

Figure S8. The produced amounts of the Cu-Zn NPs coated Ti electrode, in a CO_2 purged electrochemical cell, under bias-potential from -0.6V to -1.4V *vs.* Ag/AgCl in 1 hour.

Application of Cu-Zn NPs in photocatalytic CO_2 reduction. The Cu-Zn NPs were loaded onto the surface of a $SrTiO_3$ film using ink method. Then the film was put inside of gas purged 0.1M$KHCO_3$ solution, irradiated by UV light (Figure S9). Figure S10 showed the difference of the produced amount between CO_2 purged case and Ar purged case. HCOOH was mainly generated from CO_2 reduction. While without Cu-Zn NPs loading, pure $SrTiO_3$ film only generated small amount of CO under UV irradiation from CO_2.

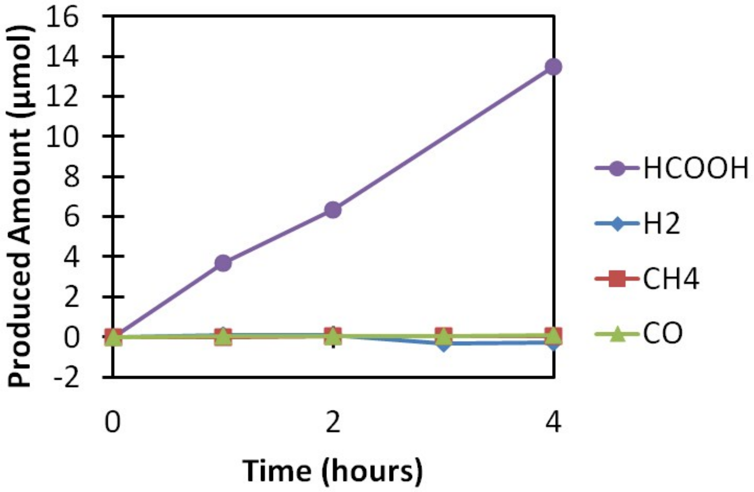

Figure S9. Produced amount of HCOOH, H_2, CH_4 and CO from Cu-Zn NPs loaded $SrTiO_3$ film under CO_2 purging with UV irradiation.

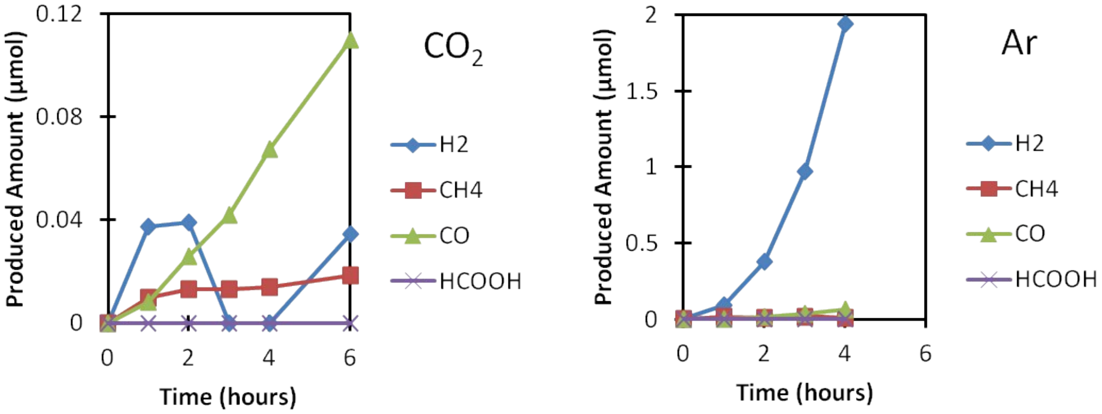

Figure S10. The produced amount of HCOOH, H_2, CH_4 and CO from pure $SrTiO_3$ film, CO_2 purging (left) and Ar purging (right) under UV irradiation.

***Operando* FT-IR spectroscopy analyses.** The in situ FT-IR spectra were measured using FTIR6100 (JASCO Ltd.), the catalytic reaction was conducted in a gas-flow reactor with a quartz window (S.T. Japan Ltd.), in which Cu-Zn NPs loaded $SrTiO_3$ powders were put in a porous ceramic cup. Pure Ar gas was introduced to the reactor at the flow rate of 100ml/min at 573 K for 1 hour as pretreatment. During the catalytic reaction at room temperature, Ar gas or CO_2 gas were introduced into the reactor through bubbling of water to flow humid gas. UV light (Hg-Xe lamp (240-300nm)), LA-410UV, Hayashi Ltd, was used as a light source. The Cu-Zn NPs loaded STO powder was prepared using ink method. The Cu NPs and Zn NPs loaded STO were prepared by chemical reduction method, through the reducing reaction of $CuCl_2$ and $ZnCl_2$ with $NaBH_4$, respectively.

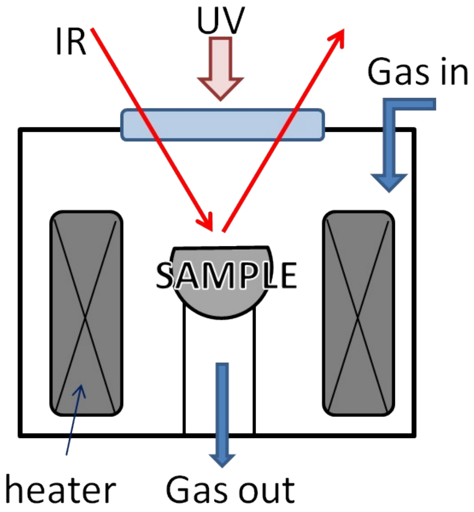

Figure S11. Schematic illustration of our *operando* FT-IR analysis system

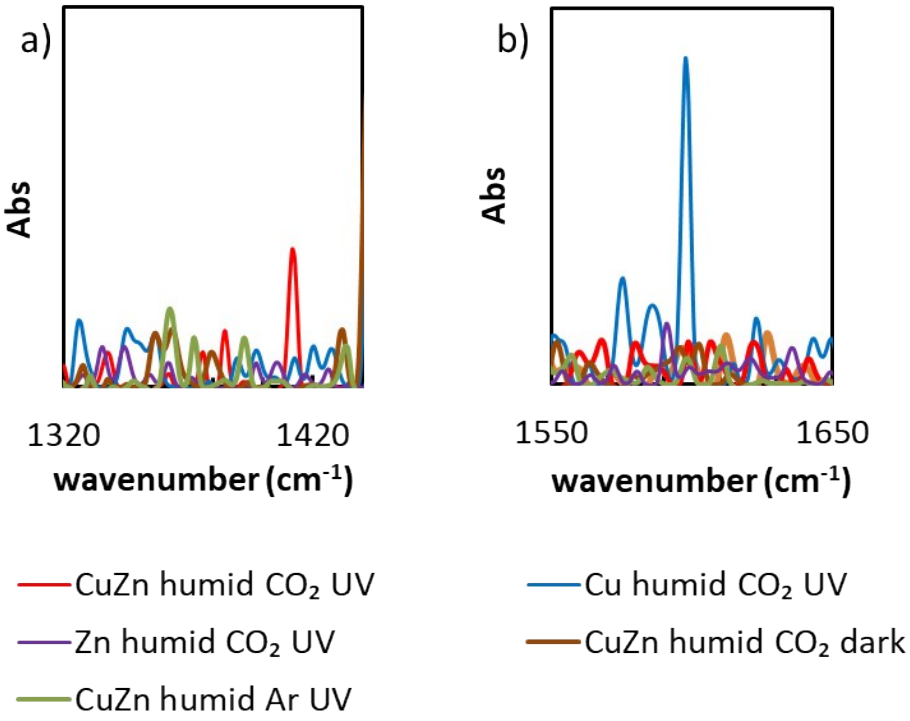

Figure S12. The *operando* FT-IR spectra of photocatalyst powders loaded by Cu-Zn NPs, pure Cu NPs and pure Zn NPs in humid CO_2 atmosphere under UV irradiation. The spectra under humid Ar with UV irradiation and under humid CO_2 in dark condition were also shown as control groups. Strontium titanate was used as a photocatalyst powder. a) and b) shows the spectra near 1400cm-1 and 1600cm-1, respectively.

(III) The characterization of the light harvesters.

Characterization of $CaFe_2O_4$ electrode. The CFO powder was successfully prepared by a solution method. After screen printing and annealing, CFO electrode was prepared. According to the XRD pattern, compared to the prepared CFO powder, the CFO electrode was highly crystallized and (hk0)-oriented.

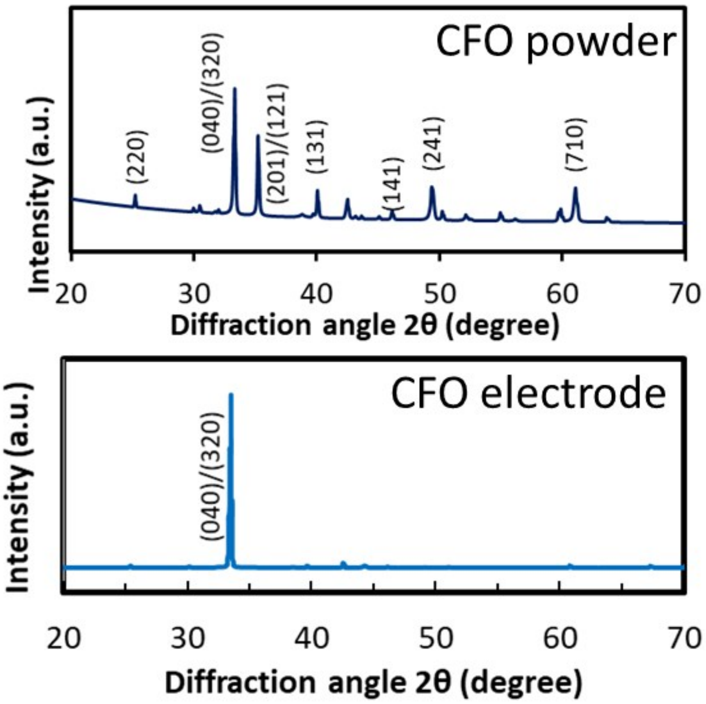

Figure S13. The XRD pattern of the prepared CFO powder and CFO electrode.

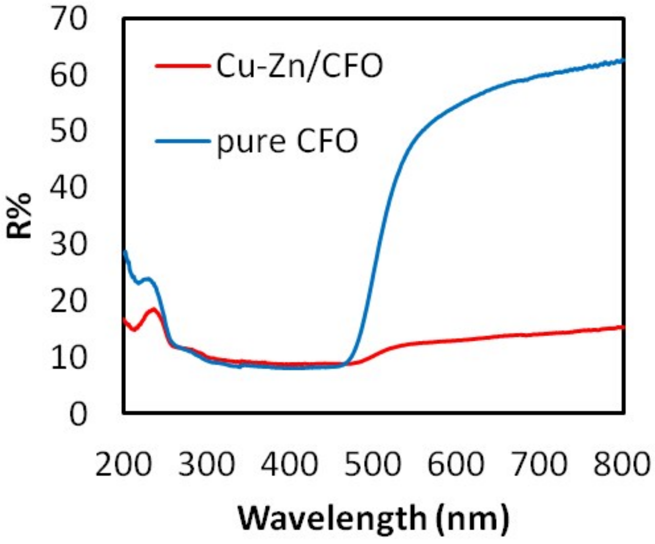

Figure S14. The UV-vis spectra of pure CFO electrode and the Cu-Zn NPs loaded CFO electrode.

Characterization of WO_3 electrode.

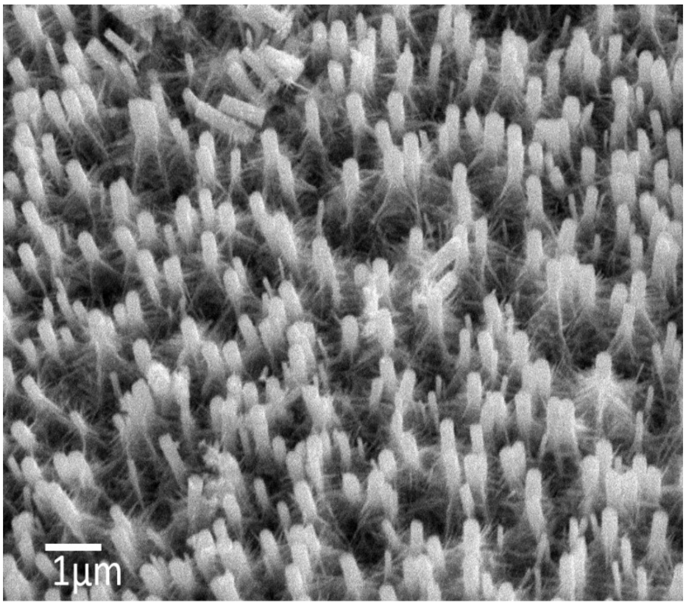

Figure S15. The SEM image of the prepared WO_3 nanotrees.

(IV) Photocatalytic performance of the CFO/WO_3 system.

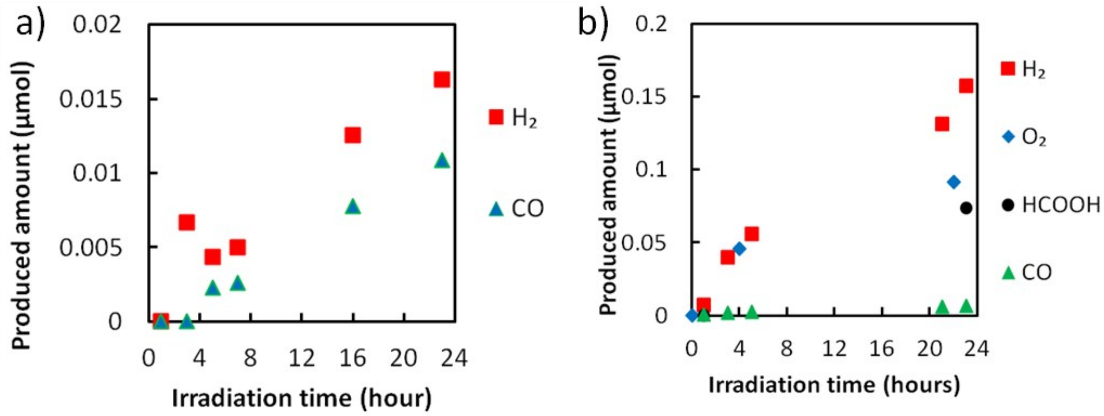

Figure S16. The produced amount of H_2, O_2, HCOOH, and CO under visible light from the photoelectrochemical cell a) Cu-Zn NPs modified CFO photocathode and WO_3 photoanode without any over-potential, the produced HCOOH amount was too small to be detected. b) using pure CFO photocathode and WO_3 as photoanode with an over-potential of -0.5V.

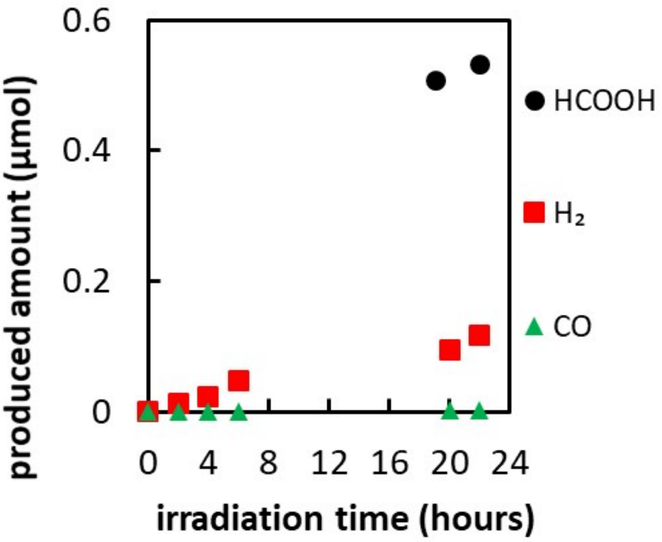

Figure S17. Repeated experiment of the produced HCOOH, H_2 and CO from the photoelectrochemical cell constructed by Cu-Zn NPs modified CFO photocathode and WO_3 photoanode, under visible light irradiation with an over-potential of -0.5V.

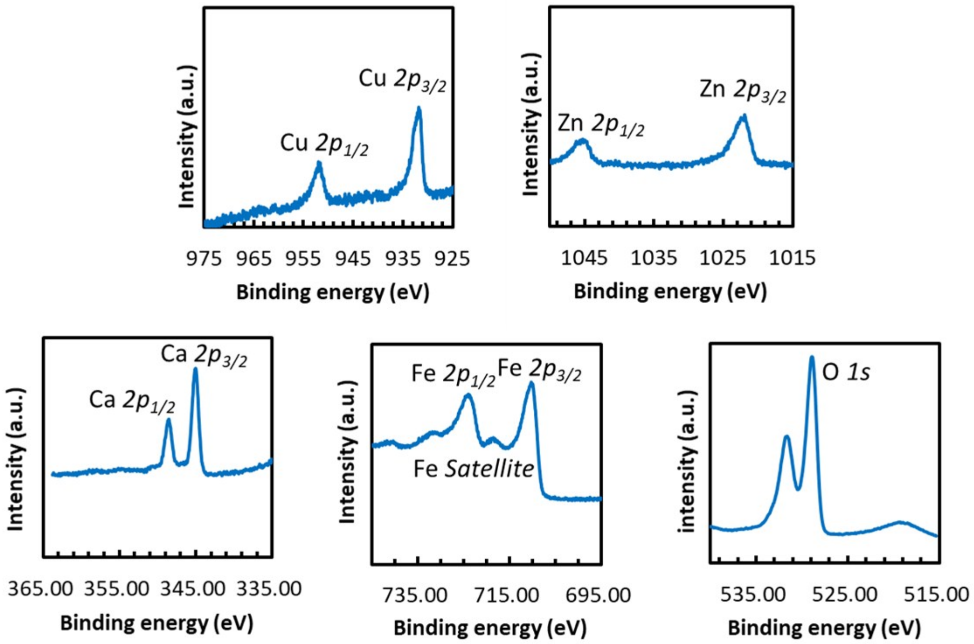

Figure S18. The HAXPES spectra of Cu *2p*, Zn *2p*, Ca *2p*, Fe *2p*, O *1s* core-levels in the Cu-Zn NPs loaded CFO electrode, after 24h photocatalytic evaluation. The Cu and Zn were not oxidized.

The calculation of the quantum efficiency:

Quantum efficiency (Φ) is defined in photocatalysis as the ratio of the rate of photocatalytic events to the absorbed photons flux within the specified wavelength range , as shown with equation Eq.S1.

$$\Phi = \frac{N_{HCOOH} + N_{H_2} + N_{CO}}{N_{absorpted\ photons}} \times 100\%$$

$$= \frac{(\gamma_{HCOOH} \times 2 + \gamma_{H_2} \times 2 + \gamma_{CO} \times 2) \times 6.025 \times 10^{23}}{\Sigma_{CFO}(Abs_{CFO} \times i_{CFO}) \times S_{CFO} + \Sigma_{WO_3}(Abs_{WO_3} \times i_{WO_3}) \times S_{WO_3}} \times 100\%$$

Eq. S1

Where γ is the generation rate of the photocatalytic products (mol/sec), *Abs* is the absorption of the CFO and WO_3, measured by UV-vis spectra. i is the photon flux intensity (1/cm^{2}sec), conversed from the illuminance of the light sources. Σ means the summing from wavelength 300nm to 800nm. S is the projected area of the photoelectrodes (cm^2). 6.025×10^{23} is the Avogadro number.

As a result,

$$\Phi = \frac{(5.51 \times 10^{-12} \times 2 + 3.09 \times 10^{-12} \times 2 + 3.27 \times 10^{-13} \times 2)}{3.52 \times 10^{15} \times 1 + 4.76 \times 10^{15} \times 0.8}$$

$= 0.14\ \%$

The calculation of the light-to-energy conversion efficiency:

Electrical bias and chemical bias from the pH difference between the cathode and anode must be considered to calculate the light-to-energy conversion efficiency as below.

The obtained chemical energy of the generated HCOOH is calculated to 0.0554 J using Eq.S.2

$$E_{HCOOH} = [HCOOH] \times 2 \times F \times (V_{form} - V_{chem\ bias} - V_{elect\ bias}) \qquad \text{Eq S.2}$$

where [*HCOOH*] is the amount of generated HCOOH (0.456 μmol); *F*: Faraday constant 96485 sA/mol; V_{form}: theoretical formation voltage for HCOOH (1.43 V); $V_{chem\ bias}$: chemical bias derived from the pH difference between two electrodes (0.30 V); $V_{elect\ bias}$: applied electrical bias (0.50 V).

The obtained chemical energy of the generated H_2 and CO was calculated by the same way, to be 0.021 J and 0.0021 J, respectively.

Then the light-to-energy conversion efficiency (η) is calculated using Eq S.3.

$$\eta = \Sigma E_{products}/E_{photon} \qquad \text{Eq S.3}$$

where E_{photon} is the integrated incident photon energy (0.001872 Wcm^{-2} × 1.8 cm^2 × (23 × 60 × 60)s =279 J).

As result, our light-to-energy conversion efficiency for the full light spectrum was calculated to be 0.028 %.